**iScience, Volume *24***

## Supplemental information

# Induction of Foxp3 and activation of Tregs by HSP gp96 for treatment of autoimmune diseases

**Yuxiu Xu, Erlong Liu, Xialin Xie, Jiuru Wang, Huaguo Zheng, Ying Ju, Lizhao Chen, Changfei Li, Xuyu Zhou, Zihai Li, Xin Li, and Songdong Meng**

# Supplementary Materials

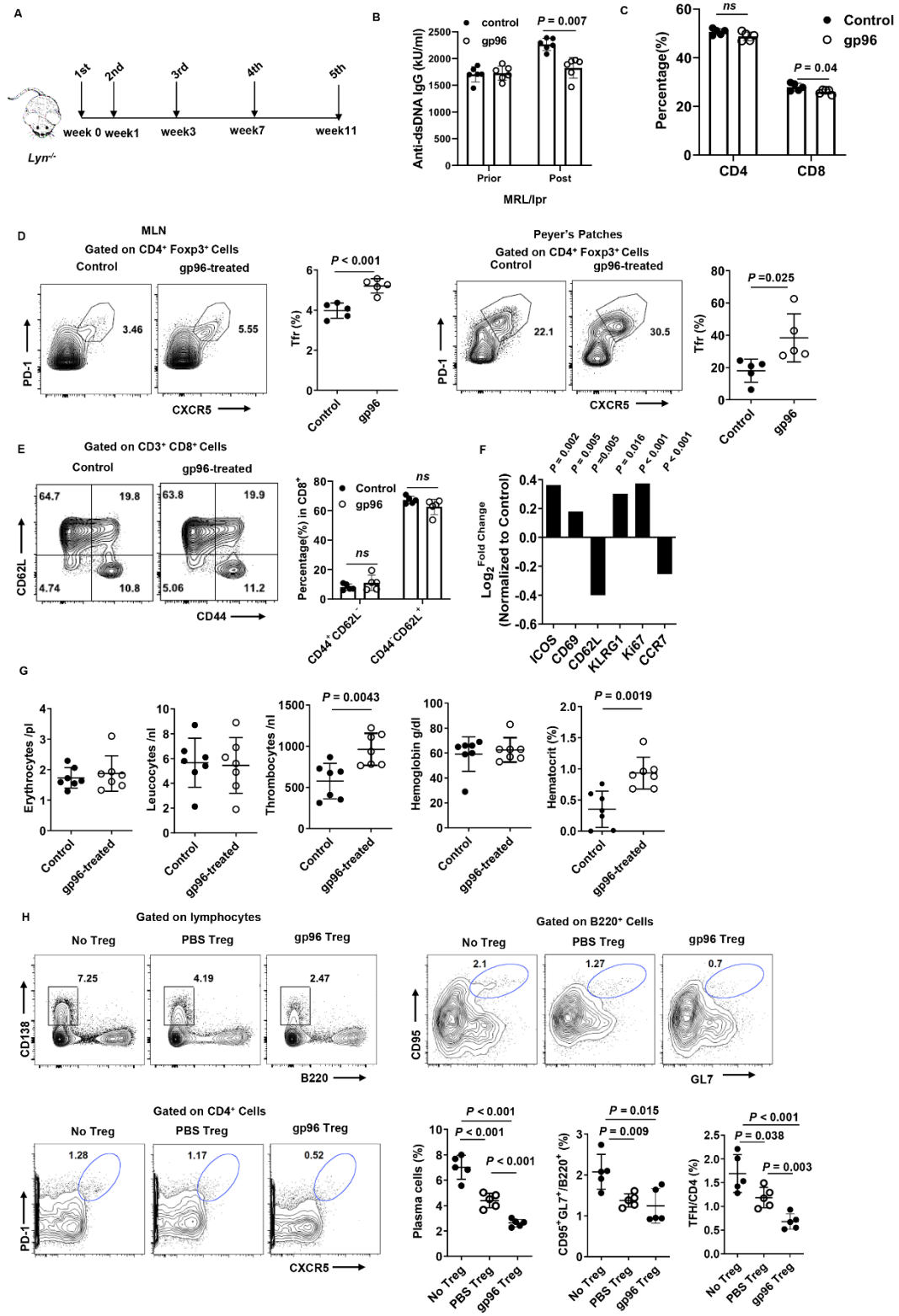


Supplementary Figure S1. Treatment of SLE by gp96 is dependent on Treg,

Related to Figure 1. Mice were immunized as in (A). (B) Serum anti-dsDNA antibodies were determined by ELISA in MRL/lpr mice one week after the last immunization. (C) FACS analysis of $CD4^+$ and $CD8^+$ percentage in spleen of *Lyn*$^{-/-}$ mice treated with gp96 or saline (control). (D) Analysis of $CXCR5^+PD\text{-}1^+Foxp3^+$ Tfr cells in the MLN and Peyer's Patches of mice immunized at 16 weeks of age. (E) Analysis of $CD8^+$ activation in spleen of *Lyn*$^{-/-}$ mice treated with gp96 or saline (control). (F) $Log_2$ fold change of ICOS, CD69, CD62L, KLRG1, Ki67 and CCR7 on Treg from gp96- or saline-treated *Lyn*$^{-/-}$ mice. (G) Analysis of peripheral blood cells in *Lyn*$^{-/-}$ mice treated with gp96 or saline (control). (H) FACS analysis of plasma cells, germinal center B cells and follicular T helper cells in the spleen of *Lyn*$^{-/-}$ mice transferred with Tregs treated as in Fig. 1K. The Student's t test was used for statistical analysis. $P$ values $< 0.05$ were considered statistically significant.

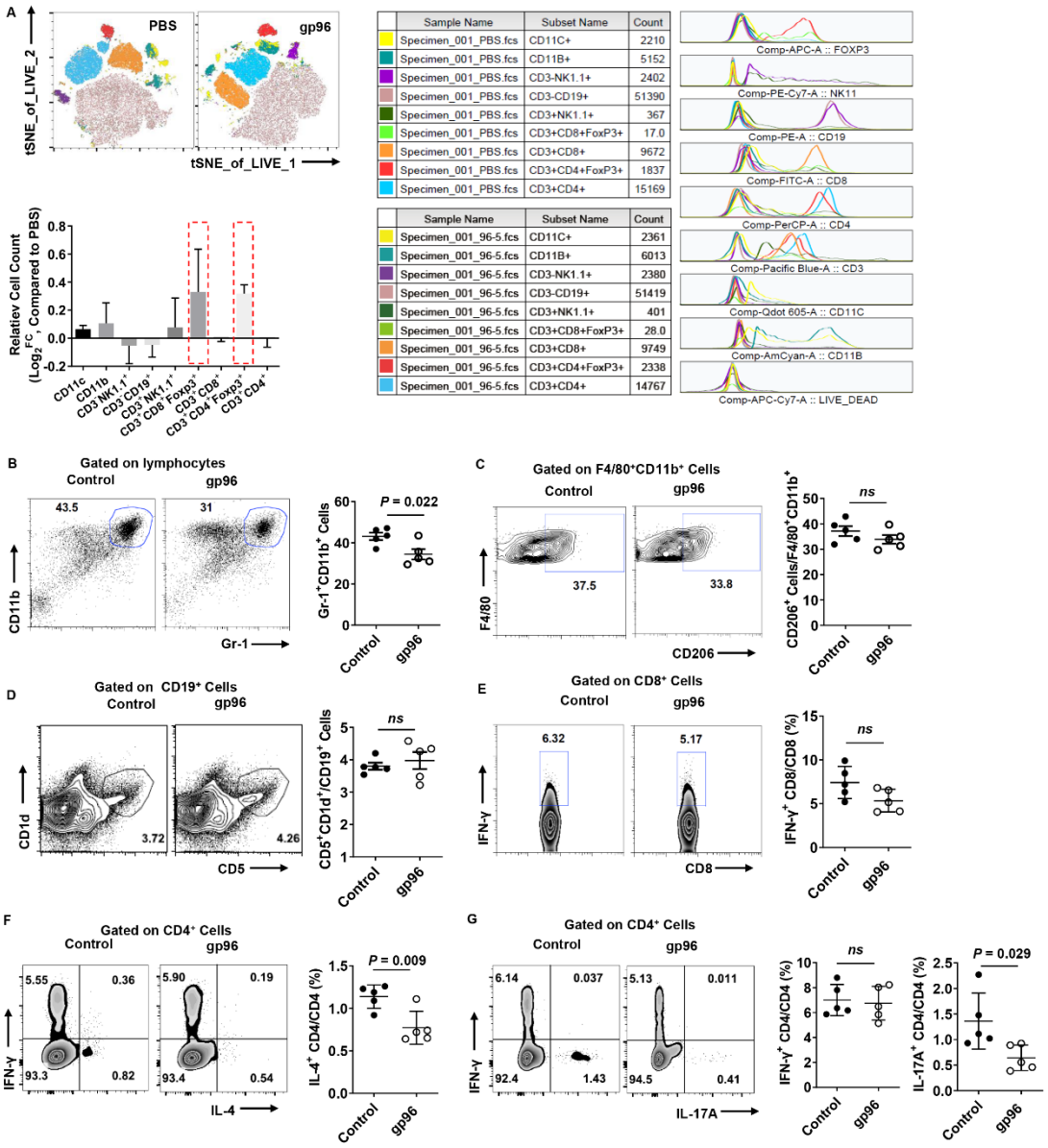


Supplementary Figure S2. Gp96 specifically upregulated Foxp3$^+$ T cells, Related to Figure 3. (A) T-distributed stochastic neighbor embedding (tSNE) plots showed distribution of lymphocyte clusters by flow cytometry. (B-D) Flow cytometry analysis of MDSC (B), M2-Macrophage (C) and regulatory B cells (D) in spleen from gp96- or saline (control)-immunized mice. (E-G) Flow cytometry analysis of IFN-γ-secreting CD8$^+$ T cells (CTL) (E), IL-4 secreting CD4$^+$ T cells (Th2) (F), IFN-γ-secreting CD4$^+$ T

cells (Th1) and IL-17A secreting $CD4^+$ T cells (Th17) (G) in spleen from gp96-or saline (control)-immunized mice. (n=5/group). The Student's t test was used for statistical analysis. *P* values $< 0.05$ were considered statistically significant. ns=not significant.

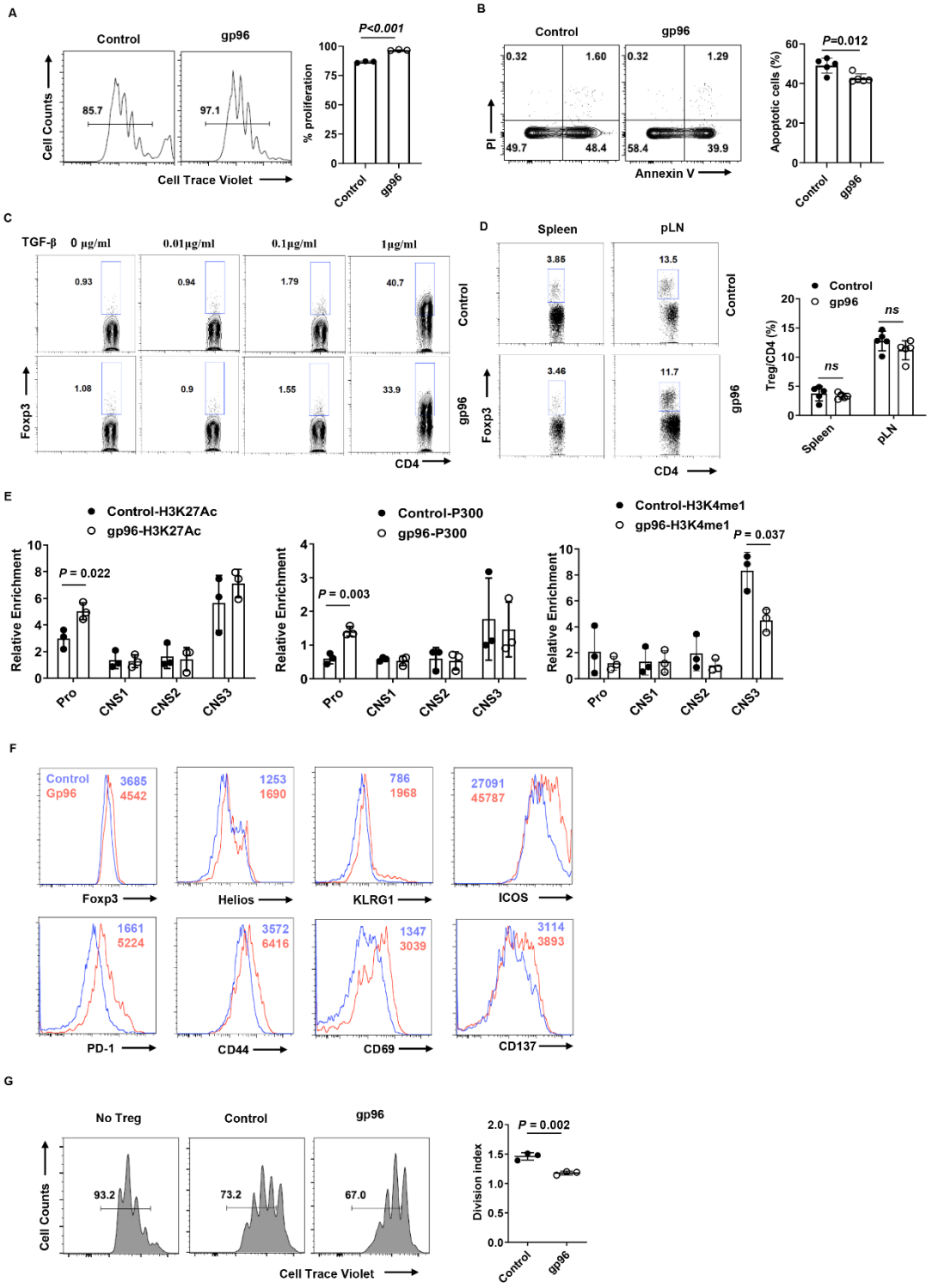


Supplementary Figure S3. Gp96 promotes Treg proliferation and suppression function, Related to Figure 3. (A) Treg cell division cycle was measured using FACS. (B) FACS analysis of Treg apoptosis by Annexin V Apoptosis Detection Kit. Annexin $V^+$ cells were counted as apoptotic

cells. (C) Naïve $CD4^+$ T cells were cultured for 3 days with different amounts of TGF-β (1, 0.1, 0.01 or 0 ng/ml) and IL-2 (100 U/ml) in the presence of saline or gp96 (100 μg/ml). Cells were then stained for Foxp3. (D) *Rag2*$^{-/-}$ mice were intravenously transferred with sorted naïve $CD4^+$ T cells from C57BL/6 mice, and then immunized with gp96 or saline for three times. Treg cells from spleen and lymph nodes were analyzed 4 weeks after the adoptive transfer. (E) ChIP analysis of H3K27ac, P300 and H3K4 monomethylation (H3K4me1) at the Foxp3 locus of Tregs. Treg cells from spleen were treated with 100 μg /ml gp96 or saline (control) for 4 h. Cell lysates were immunoprecipitated with anti-H3K27ac, anti-P300 or anti-H3K4me1 antibodies, followed by real-time PCR analysis. (F) FACS analysis of markers on Treg. Sorted Treg were cultured for 3 days with Dynabeads$^{TM}$ mouse T-activator CD3/CD28 and IL-2 (2000U/ml) in the presence of saline (control) or gp96 (100 μg/ml). Red line, gp96. Blue line, control. (G) A total of $5\times10^4$ cell trace violet-labeled $CD4^+CD25^-$ Teff cells were cultured with Tregs at a ratio of 4:1 for 3 days. Teff cell division cycle was measured using FACS (left). Division index was calculated (right). The Student's t test was used for statistical analysis. *P* values < 0.05 were considered statistically significant. ns=not significant.

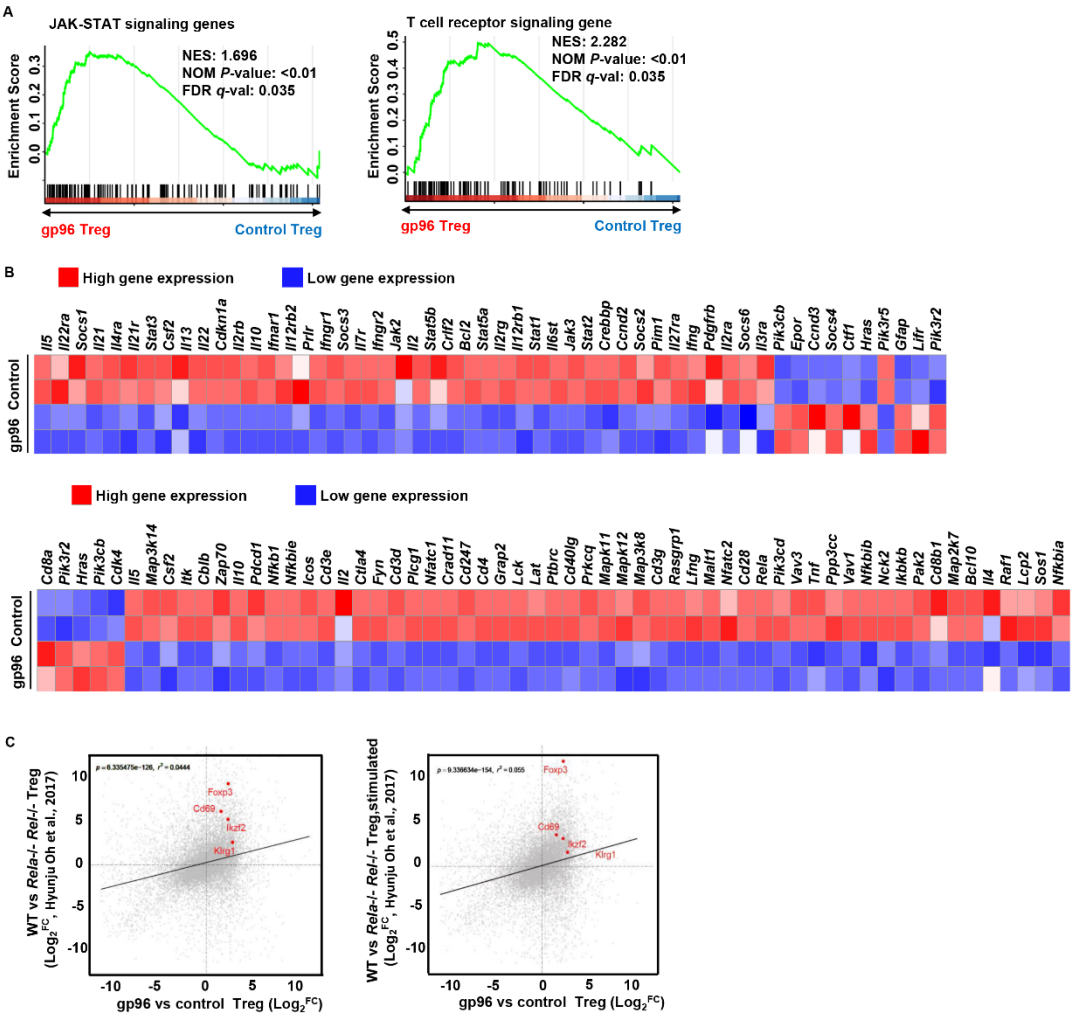


Supplementary Figure S4. Treg signature gene expression changes by gp96 are related to p65 and c-Rel, Related to Figure 5. (A) Gene set enrichment analysis (GSEA) of JAK-STAT signaling and T cell receptor signaling gene set in gp96-treated Foxp3-Cre Treg cells relative to expression in control Treg cells. (B) Heatmap of JAK-STAT signaling and T cell receptor signaling pathways ($Log_2$ fold change) that are differentially expressed. (C) $Log_2$ fold changes of gp96-treated Treg versus control Treg and unstimulated *Rela*$^{-/-}$*Rel*$^{-/-}$ (DKO) versus unstimulated WT Treg (Left) and $Log_2$ fold changes of gp96-treated Treg versus control Treg and stimulated *Rela*$^{-/-}$*Rel*$^{-/-}$ (DKO) versus stimulated WT Treg (Right) were plotted.

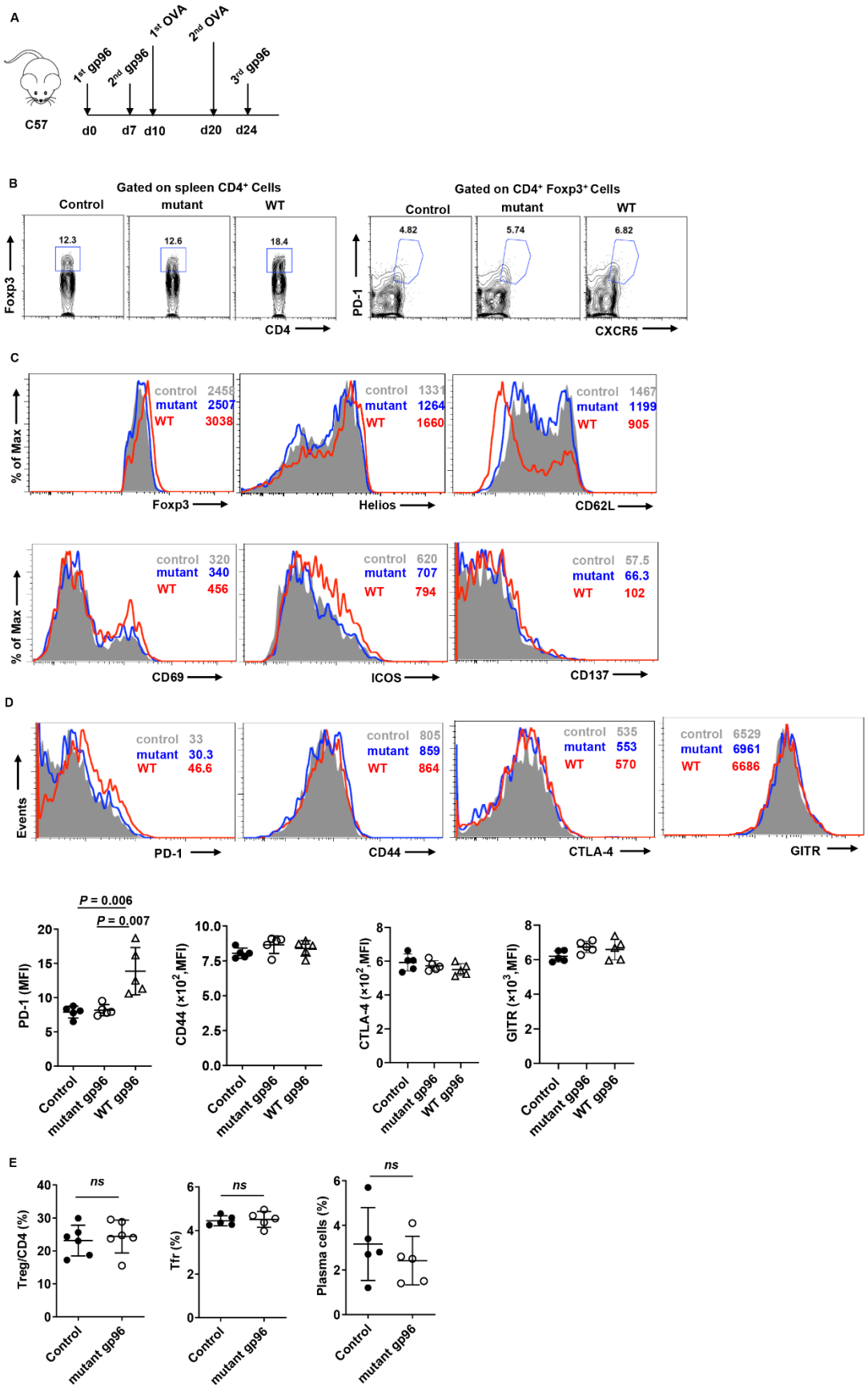


Supplementary Figure S5. Activation of Treg by gp96 requires TLRs

binding domain, Related to Figure 6. (A) C57BL/6 mice were immunized with 200 μg wide-type gp96 (WT) or mutant gp96 or saline as control and treated with NP-OVA (n=5/group). (B) FACS analysis of Treg cells and Tfr cells in spleen. (C) Mean fluorescence intensity (MFI) of the indicated markers as in Fig.6E. (D) FACS analysis and mean fluorescence intensity (MFI) of PD-1, CD44, CTLA-4, GITR. (E) FACS analysis of $CD4^{+}Foxp3^{+}$ Treg, Tfr and plasma cells in spleen of *Lyn*$^{-/-}$ mice. The Student's t test was used for statistical analysis. *P* values < 0.05 were considered statistically significant. ns=not significant.

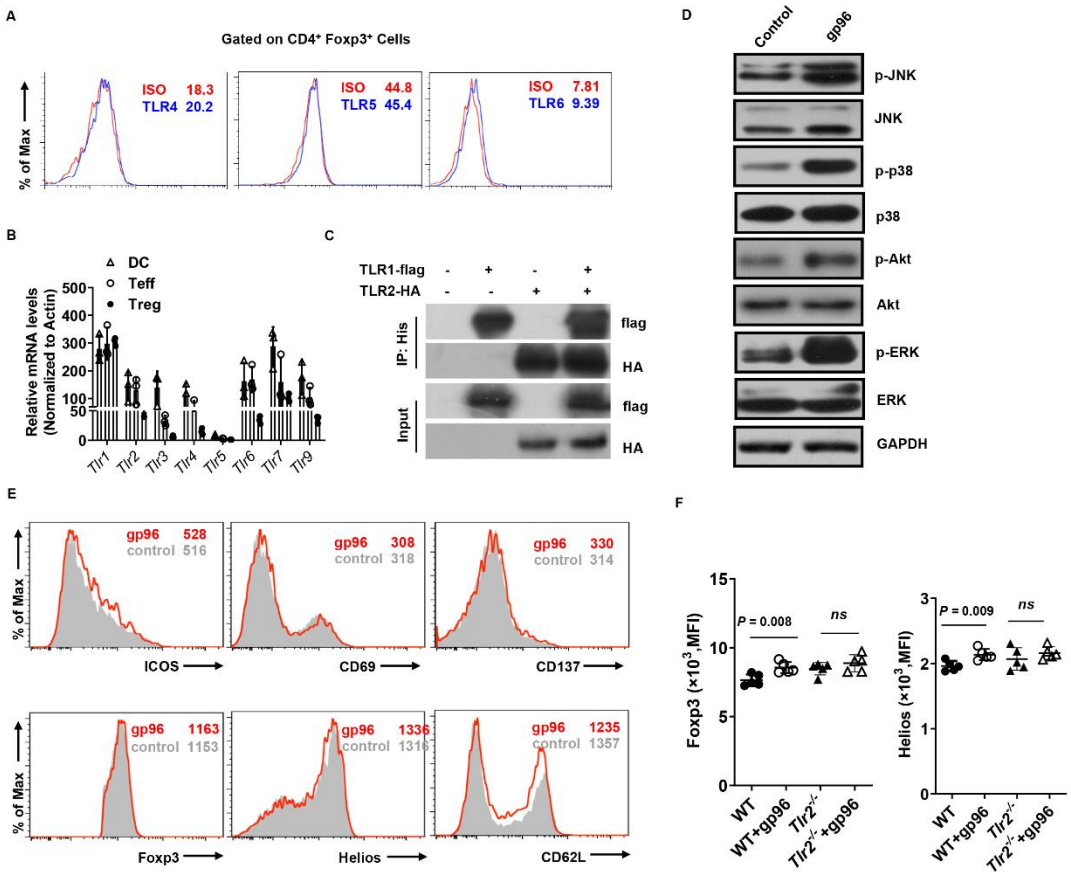


Supplementary Figure S6. Gp96 activates TLR2 down-stream pathway,

Related to Figure 6. (A) FACS analysis of surface TLR4/5/6 expression in $CD4^+Foxp3^+$ Tregs from C57BL/6 mice. (B) Real-time PCR analysis of different TLRs expression in $CD11c^+$ DC cells, $CD4^+Foxp3^-$ Teff cells and $CD4^+Foxp3^+$ Tregs. (C) 293T cells were co-transfected with an empty vector, TLR1-FLAG, TLR2-HA or both TLR1-FLAG and TLR2-HA for 48 h. Cells were cultured with 100 μg/ml His-gp96 for additional 4 h before subjected to immmoprecipitation with anti-His antibody and western blotting. (D) Western blot of JNK, p38, Akt and ERK phosphorylation in Treg cells treated with 100 μg/ml of gp96 or saline (control). (E) Flow cytometry analysis of ICOS, CD69, CD137, Foxp3, Helios and CD62L expression on $CD4^+Foxp3^+$ Tregs in the spleen from *Tlr2*$^{-/-}$ mice immunized with 200 μg gp96 or saline (control) (n=5/group). (F) Flow cytometry analysis of Foxp3 and Helios expression on $CD4^+Foxp3^+$ Tregs from $CD45.1^+$ cells and $CD45.2^+$ cells as in Fig.6M.

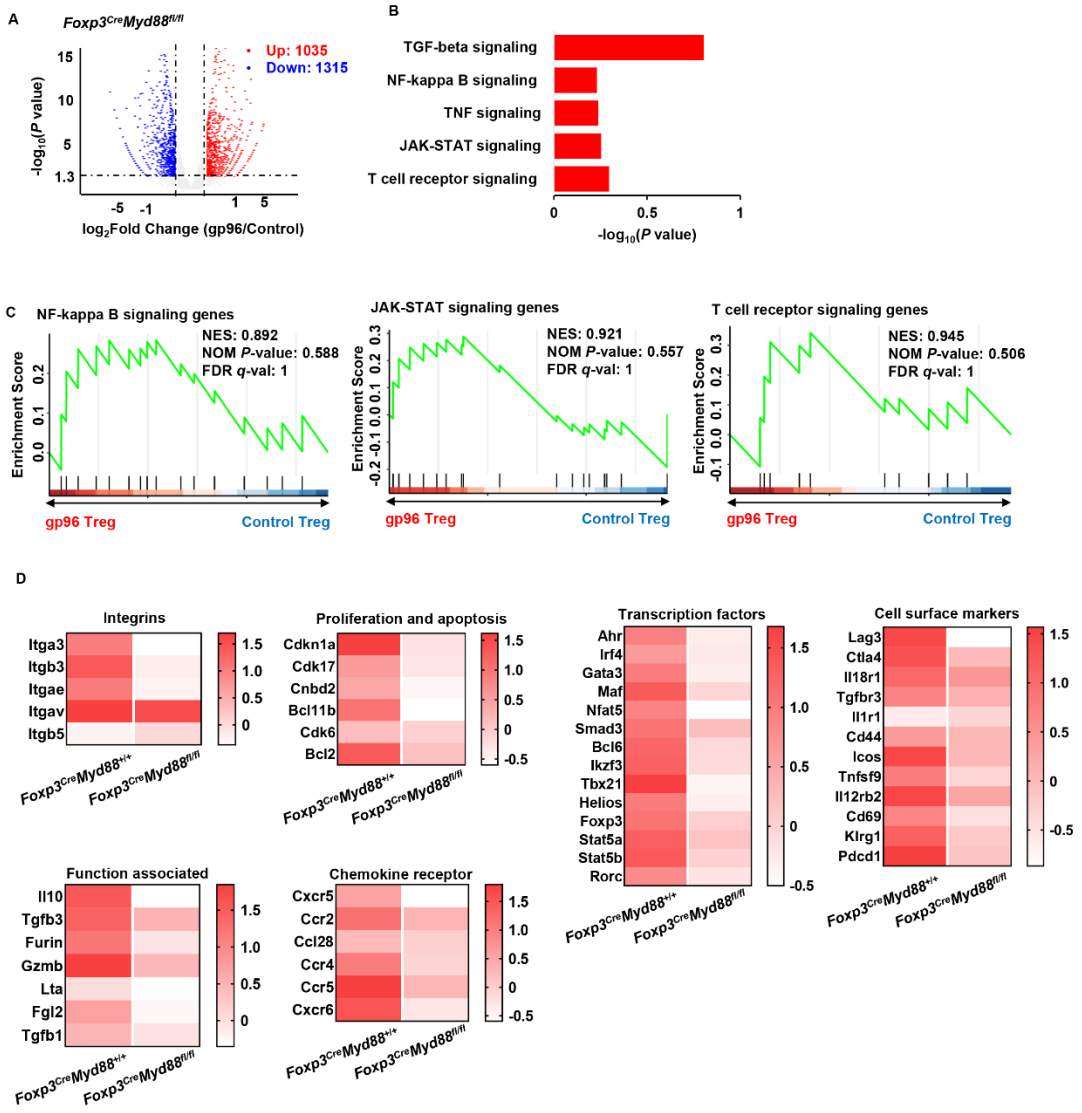


Supplementary Figure S7. MyD88 signaling is essential for gp96-induced Treg signature gene expression changes, Related to Figure 7. (A) Global gene expression in Treg cells from gp96-immunized *Foxp3*$^{Cre}$*Myd88*$^{fl/fl}$ mice vs. from saline-treated *Foxp3*$^{Cre}$*Myd88*$^{fl/fl}$ numbers in plots indicate genes up-regulated (red) or down-regulated (blue) by twofold or more ($P < 0.05$). (B) Gene Ontology (GO) terms of the differentially expressed genes. (C) Gene set enrichment analysis (GSEA) of NF-κB signaling, JAK-STAT signaling and T cell receptor signaling gene set. (D) Heat map of

Treg signature genes in *Foxp3*$^{Cre}$*Myd88*$^{+/+}$ and *Foxp3*$^{Cre}$*Myd88*$^{fl/fl}$ mice. Relative gene expression levels were shown as $Log_2$ fold changes in gp96-immunized mice relative to control mice.

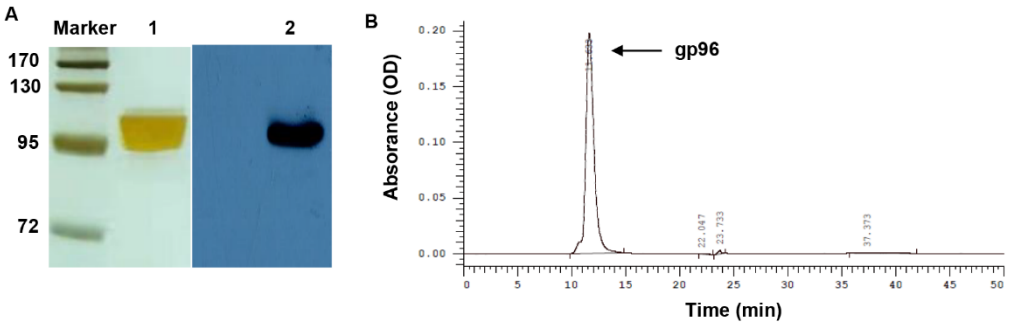


Supplementary Figure S8. Purification of recombinant gp96, Related to the STAR Methods. (A) The purified recombinant gp96 preparations were subjected to SDS-PAGE and silver nitrate staining (lane 1) or immunobloted with anti-gp96 Ab (lane 2). (B) HPLC analysis of recombinant gp96. The purity of recombinant protein was determined by HPLC and showed a specific peak at about 12 minutes.

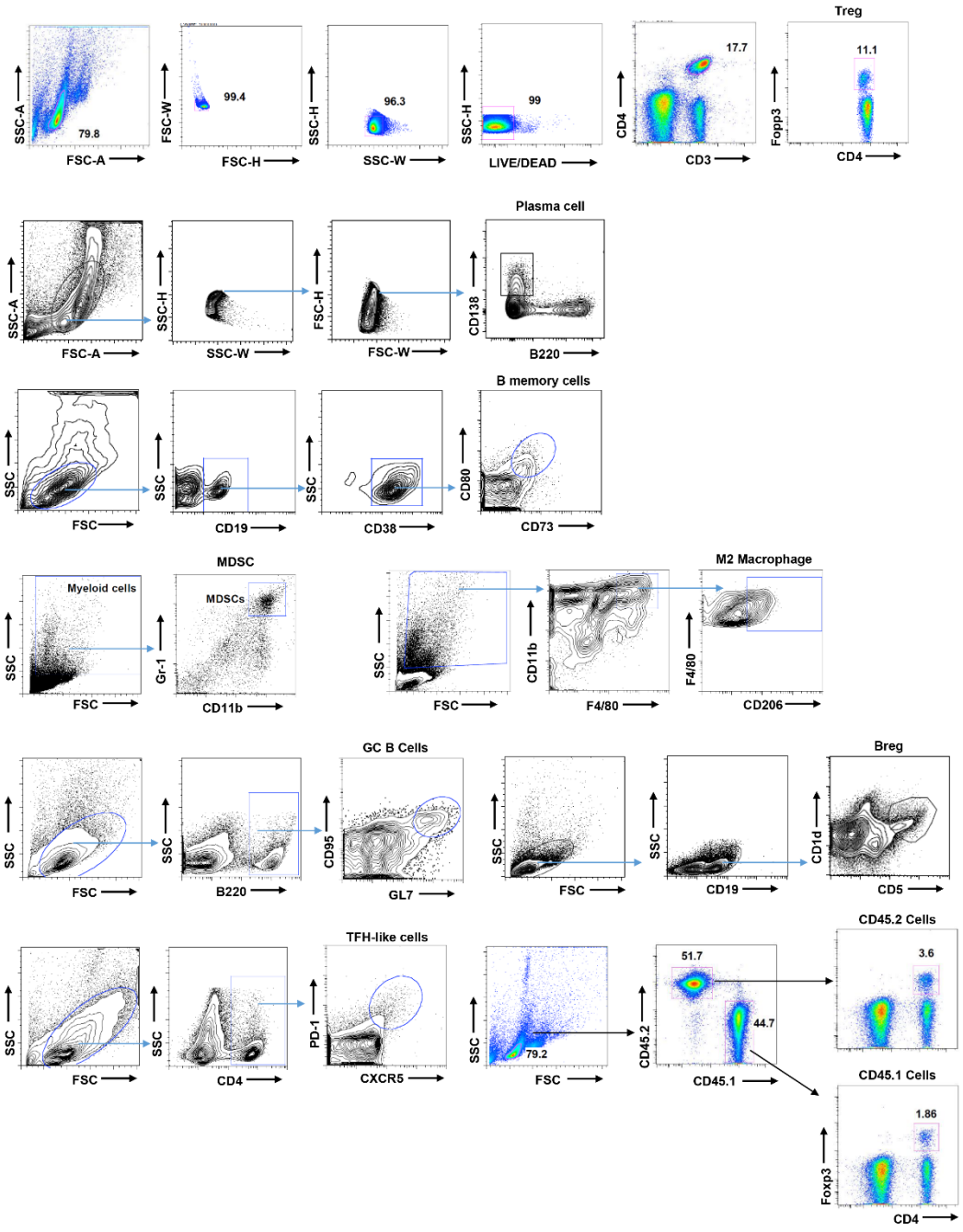


Supplementary Figure S9. Flow cytometry gating strategy for immune cell identification used in this article, Related to Figure 1.

Table S1. List of primers used in reverse transcription quantitative PCR (RT-qPCR) (Related to STAR Methods).

| **Primers** | **Sequence (5′-3′)** |
|---|---|
| *Foxp3*-Forward (F) | GGCCCTTCTCCAGGACAGA |
| *Foxp3*-Reverse (R) | GCTGATCATGGCTGGGTTGT |
| *Tlr1*-F | GCATGATTCTGCCTGGGTGAAG |
| *Tlr1*-R | GGAATGGGTGCCAGCAAGATG |
| *Tlr2*-F | AAGAGGAAGCCCAAGAAAGC |
| *Tlr2*-R | GAAGTCAGGAACTGGGTGGAG |
| *Tlr3*-F | ACCCTCTGTGCAGAAGATTCA |
| *Tlr3*-R | GCTGAATTCCGAGATCCAAG |
| *Tlr4*-F | AAACTTGCCTTCAAAACCTGGC |
| *Tlr4*-R | ACCTGAACTCATCAATGGTCACATC |
| *Tlr5*-F | CGAGTGAGGTCAGTCCTGGA |
| *Tlr5*-R | GTCTGGAGAGGCTCATGCTAAG |
| *Tlr6*-F | CCTGGTATGTGAGGATGCTGTGTC |
| *Tlr6*-R | GAGACAGCACAAAGATGGCCTTG |
| *Tlr7*-F | CTGTCTCAGAGGACTCCATCTATAG |
| *Tlr7*-R | GTCAGAGATAGGCCAGGATCATC |
| *Tlr9*-F | CTGGTACTGTTTTCATCTGTGCC |
| *Tlr9*-R | CAGCTCGTTATACACCCAGTC |
| *Actb*-F | CGCCACCAGTTCGCCATGGA |

| | |
|---|---|
| *Actb*-R | TACAGCCCGGGGAGCATCGT |
| **For detection of methylation and acetylation** | **Sequence (5′-3′)** |
| *Foxp3* promoter-F | TAATGTGGCAGTTTCCCACAAGCC |
| *Foxp3* promoter-R | AATACCTCTCTGCCACTTTCGCCA |
| *Foxp3* CNS1-F | AGACTGTCTGGAACAACCTAGCCT |
| *Foxp3* CNS1-R | TGGAGGTACAGAGAGGTTAAGAGCCT |
| *Foxp3* CNS2-F | ATCTGGCCAAGTTCAGGTTGTGAC |
| *Foxp3* CNS2-R | GGGCGTTCCTGTTTGACTGTTTCT |
| *Foxp3* CNS3-F | TCTCCAGGCTTCAGAGATTCAAGG |
| *Foxp3* CNS3-R | ACAGTGGGATGAGGATACATGGCT |
| *Hsp90ab1*-F | TTACCTTGACGGGAAAGCCGAGTA |
| *Hsp90ab1*-R | TTCGGGAGCTCTCTTGAGTCACC |
| *Rpl30*-F | TCGGCTTCACTCACCGTCTTCTTT |
| *Rpl30*-R | TGTCCTCTGTGTATGCTAGGTTGG |
| *Hspa2*-F | TCGTGGAGAGTTGTGAGAAGCGA |
| *Hspa2*-R | AACGTTAGGACGAAAGCGTCAGGA |
| *Gm5069*-F | TAAGCAATTGGTGGTGCAGGATGC |
| *Gm5069*-R | AAAGGGTCATCATCTCCGTCCGTT |
| **For detection of FoxO1 binding** | **Sequence (5′-3′)** |

| | |
|---|---|
| *Foxp3* CNS1-F | CCCTGCAATTATCAGCACAC |
| *Foxp3* CNS1-R | TGTGGGAAACTGCCACATTA |
| *Foxp3* CNS2-F | GGTGGGAAAGTGGGCTATCT |
| *Foxp3* CNS2-R | ATGCACAGAGGGAATGGAAT |
| *Foxp3* CNS3-F | ATCTGGCCAAGTTCAGGTTG |
| *Foxp3* CNS3-R | GGCGTTCCTGTTTGACTGTT |
| **For detection of c-Rel/p65 binding** | **Sequence (5′-3′)** |
| Promoter NFKB-F | CCCTCTAGCAGTCCACTTCACCAA |
| Promoter NFKB-R | AATACCTCTCTGCCACTTTCGCCA |
| CNS3 NFKB-1-F | TTTGCATGGTAGCCAGATGGACG |
| CNS3 NFKB-1-R | AGGTTTCGTTCCGAGAAGTGGCTA |
| CNS3 NFKB-2-F | TTTGCATGGTAGCCAGATGGACG |
| CNS3 NFKB-2-R | AGGTTTCGTTCCGAGAAGTGGCTA |
| CNS3 NFKB-3-F | TCCCAGAAACAACCTCCATACAGC |
| CNS3 NFKB-3-R | TGTCTAGTGGTACTAGGGACCTGGA |